STRUCTURAL CONTROL AND HEALTH MONITORING
Struct. Control Health Monit. 2004; **11**:55–74 (DOI: 10.1002/stc.32)

Probability and sensitivity analysis of strain measurements in FRP

Alfred Strauss[1,*,†], Giovanni Pascale[2], Barbara Bonfiglioli[2], Konrad Bergmeister[1] and Paola Di Muro[3]

[1] *IKI, Department of Structural Engineering, University of Boku, Vienna, Austria*
[2] *DISTART, Department of Structural Engineering, University of Bologna, Bologna, Italy*
[3] *Mathematics and Computer Science Department, University of Brandon, Brandon, Manitoba, Canada*

SUMMARY

Monitoring is an important issue for FRP strengthening systems in order to control their health state. Strain gauges are often used for this aim, but the measures to be utilised can be affected by various factors. In this paper the influence of various factors is taken into account, such as the characteristics of resin coating, the type of glue and the gauge length. The theoretical approach developed in previous work performed on a deterministic basis is extended here to the probabilistic field. The objective is to make a sensitivity analysis of the basic variables which can cause errors in strain measurements. Additionally, the effect of the deviation of the direction of the gauges from the longitudinal direction of the FRP sheets is considered and the existing approach is extended to take this into account. Copyright © 2004 John Wiley & Sons, Ltd.

KEY WORDS: probability approach; sensitivity analysis; strain measurement; fibre-reinforced polymer; electrical strain gauges

1. INTRODUCTION

Fibre-reinforced polymer (FRP) sheets and laminates are frequently used in the rehabilitation of civil structures, in particular for externally bonded strengthening. The assessment of the effectiveness of the system is usually based both on preliminary laboratory tests on the materials, and on non-destructive or semi-destructive surveys on site after application [1]. Several procedures can be adopted for structural health monitoring during the service life, which can be based both on periodical control of the structural global behavior, e.g. with dynamic testing [2] or on the use of sensors permanently placed on the strengthened structure. The readings provided by the sensors can be periodically collected in place or remotely acquired [3]. This research deals with strain sensors. Strain measurements can be carried out by traditional sensors, such as electrical strain gauges (ESG), or by innovative fibre optic sensors

*Correspondence to: Alfred Strauss, IKI, Department of Structural Engineering, University of Boku, Vienna 1190, Austria.
† E-mail: alfred.strauss@iki.boku.ac.ak

Received 6 February 2003
Revised 26 July 2003
Accepted 20 August 2003

(FOS) [4–6]. The strain measurements can be affected by various factors, such as the type, mechanical properties, and thickness of the adhesive film, or the characteristics of the surface.

The application of strain gauges on concrete, owing to the roughness of the surface, can display successful results if a suitable adhesive type and gauge length are selected. Furthermore, it can be assumed that the location of the strain gauges influences the strain measurements. When strain measurements are to be carried out on externally bonded FRP strengthening, the ESG are usually glued onto the surface of the composite. Nevertheless, the use of electrical strain gauges on FRP composites must be evaluated with meticulously. A mathematical model has been developed to simulate the influence of various parameters on strain measurement [2, 7]. The model takes into account the interaction between three layers: FRP, resin coating; and the gauge adhesive. The analytical results show that the value is affected by several factors: the coating thickness; resin elastic modulus; gauge length and the type of adhesive used to bond the gauge. The experimental results are quite varied for the FRP specimens [7]. The target of this research is to evaluate this mathematical model on the basis of a probabilistic formulation and to find out the sensitivity of the participated variables used in the model. In this paper the probabilistic theoretical approach is described and evaluated for the data that are available.

A further point of view within these examinations is the consideration of the possible deviation of the electrical strain gauge's axis from the longitudinal axis of the FRP. Therefore, the mathematical formulation is extended and the additional basic variables are included in the sensitivity analysis.

This research should allow the inclusion of the uncertainties of the variables which are used for the determination of the measurement error of gauges and should also provide us with a tool for improving predictions of the behaviour of strengthened structures.

2. STRAIN MEASUREMENT PROBLEMS IN FRP

2.1. Mathematical formulation of the deterministic model

The model studied is shown in Figure 1. It represents a FRP specimen in tension, with resin coating layers at both sides. Two strain gauges are bonded to it, on opposite sides. Because of the symmetry, only a quarter of the model was studied.

In Figure 2 the force P and the shear stresses τ acting on the layers are shown, for a differential section. Figure 3 represents the deformations and the displacements of the layers.

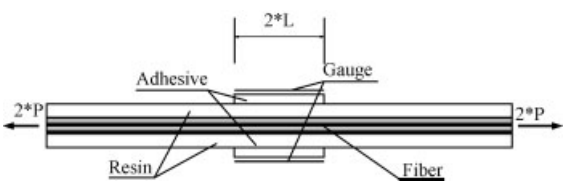

Figure 1. Laminate with coating layers and strain gauges bonded.

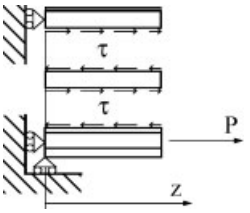

Figure 2. Forces and stresses acting on the layers.

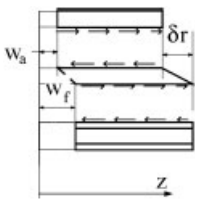

Figure 3. Deformations of layers.

Table I. Symbols adopted in this work.

Symbol	Description	Symbol	Description
L	Half gauge length	E_f	Young's modulus of fibre
N_f,	Axial force on fibre	E_r	Young's modulus of resin
N_a	Axial force on adhesive	E_a	Young's modulus of adhesive
t_f	Thickness of fibre layer	G_r	Shear modulus of the resin
t_r	Thickness of resin layers	z	Distance from centre
t_a	Thickness of adhesive layers	dz	Differential length
b_f	Width of fibre layer	τ	Shear stress at the interface
b_r	Width of resin layers	w_f	Longitudinal displacement of fibre
b_a	Width of adhesive layers	w_a	Longitudinal displacement of adhesive
P	One-quarter of applied load	δ	Relative displacement between lower and upper bound of the resin layer

The following hypotheses are accepted:

- fibre, resin and adhesive are all orthotropic and have linear elastic behaviour;
- thermal variations do not occur;
- the shear stress at the interface between the fibre and resin is equal to the shear stress at the interface between the resin and adhesive;
- the axial force in the resin is neglected;
- only shear strain is present in the resin layer;
- only axial strain is present both in the fibre and in the adhesive layer.

Symbols are adopted as detailed in Table I.
The compatibility condition of the longitudinal displacements is:

$$w_f(z) = w_a(z) + \delta_r(z) \tag{1}$$

The terms of Equation (1) can be expressed as

$$w_f(z) = \int_0^z \frac{N_f(z)}{E_f b_f t_f} dz \qquad w_a(z) = \int_0^z \frac{N_a(z)}{E_a b_a t_a} dz \qquad \delta_r(z) = \frac{t_r}{G_r} \tau(z) \tag{2}$$

The axial force in the fibre and in the adhesive, respectively, are

$$N_f(z) = P - b_f \int_z^L \tau(z)\, dz \qquad N_a(z) = P - N_f(z) \tag{3}$$

By substituting the values of Equation (2) in Equation (1) and taking into account the expression for N_a provided by Equation (3), the following equation is obtained:

$$\left(\frac{1}{E_f t_f b_f} + \frac{1}{E_a t_a b_a}\right) \int_0^z N_f(z)\, dz = \frac{Pz}{E_a t_a b_a} + \frac{t_r}{G_r} \tau(z) \tag{4}$$

By differentiating Equation (4) twice the following differential equation is derived:

$$\tau''(z) - \alpha^2 \tau(z) = 0 \tag{5}$$

where:

$$\alpha = \sqrt{\frac{G_r}{t_r}\left(\frac{1}{E_f t_f b_f} + \frac{1}{E_a t_a b_a}\right) b_f} \tag{6}$$

The solution of Equation (5) can be expressed as:

$$\tau(z) = C_1 \sinh(\alpha x) + C_2 \cosh(\alpha x) \tag{7}$$

where C_1 and C_2 are constants which can be calculated by introducing the following boundary conditions

$$\tau(0) = 0 \tag{8}$$

$$N_f(L) = P \tag{9}$$

So, the final solution is:

$$\tau(z) = \frac{PG_r}{E_f b_f t_f t_r \alpha \cosh(\alpha L)} \sinh(\alpha z) \tag{10}$$

By substituting Equation (10) in Equation (4), the strain in the fibre and in the adhesive can be written as:

$$\varepsilon_a(z) = \frac{N_a(z)}{E_a t_a b_a} \qquad \varepsilon_f(z) = \frac{N_f(z)}{E_f t_f b_f} \tag{11}$$

or

$$N_f(z) = \varepsilon_f(z) E_f A_f$$

$$N_a(z) = \varepsilon_a(z) E_a(\text{var}) A_a$$

where E_a has to be established experimentally and A_f and A_a represent the section area of the fibre and adhesive layers, respectively.

The strain ratio

$$r = \frac{\varepsilon_a}{\varepsilon_f}$$

is finally derived, which is useful to evaluate the error in strain measurement due to the shear deformation of the resin. This is a function of various factors, such as the thickness of the layers of resin and adhesive, the gauge length and the values of Young's modulus of the materials.

3. EVALUATION OF THE PROBABILISTIC MODEL FOR THE ELECTRICAL STRAIN GAUGE

In this paragraph the extension of the mathematical model based on the probabilistic approach is presented.

3.1. Modelling concept

The treatment of the measuring errors on a probabilistic basis needs a formulation of a limit state function or response function. The response function (Equation 12), offers a solution for the problem discussed. It is the deterministic formulation, as already derived in the Section 2.1, for the strain ratio error by measurement with ESG. The closed-form solution of the deterministic equation provided an exact result, but neither the input quantities nor the results can be determined exactly.

$$r(z) = \frac{\varepsilon_a(z)}{\varepsilon_f(z)} = \frac{-b_f \int_z^L \dfrac{PG_r}{E_f b_f t_f t_r \sqrt{\dfrac{G_r}{t_r}\left(\dfrac{1}{E_f t_f b_f}+\dfrac{1}{E_a t_a b_a}\right) b_f} \cosh\left(\sqrt{\dfrac{G_r}{t_r}\left(\dfrac{1}{E_f t_f b_f}+\dfrac{1}{E_a t_a b_a}\right) b_f L}\right)} \sinh\left(\sqrt{\dfrac{G_r}{t_r}\left(\dfrac{1}{E_f t_f b_f}+\dfrac{1}{E_a t_a b_a}\right) b_f z}\right) dz}{E_a t_a b_a}}{\dfrac{P - b_f \int_z^L \dfrac{PG_r}{E_f b_f t_f t_r \sqrt{\dfrac{G_r}{t_r}\left(\dfrac{1}{E_f t_f b_f}+\dfrac{1}{E_a t_a b_a}\right) b_f} \cosh\left(\sqrt{\dfrac{G_r}{t_r}\left(\dfrac{1}{E_f t_f b_f}+\dfrac{1}{E_a t_a b_a}\right) b_f L}\right)} \sinh\left(\sqrt{\dfrac{G_r}{t_r}\left(\dfrac{1}{E_f t_f b_f}+\dfrac{1}{E_a t_a b_a}\right) b_f z}\right) dz}{E_f t_f b_f}} \tag{12}$$

For the probabilistic consideration of this problem, distribution functions are assigned to the ten variables which appear in Equation (12). The distribution functions, together with the statistical moments define the ranges for the input values, or in other words, the uncertainties of the input values (random variables) are defined. The random variables and the descriptive elements are represented in Figure 4(a). As is evident in Figure 4(b) a normal distribution was accepted for all random variables since detailed examinations are missing regarding the distribution types. For the evaluation of the response function the first-order, second-moment method (FOSM) was used [8].

This method is included in the software package VaP which will be briefly described later. With this method, the answer function delivers for r a random variable. Owing to the uncertainties in the input, uncertainties also have to appear in the result. Therefore, the description of the result r is meaningful and realistic. It is, however, possible to influence the uncertainty of the result efficiently if uncertainties, belonging to the input quantities, can be

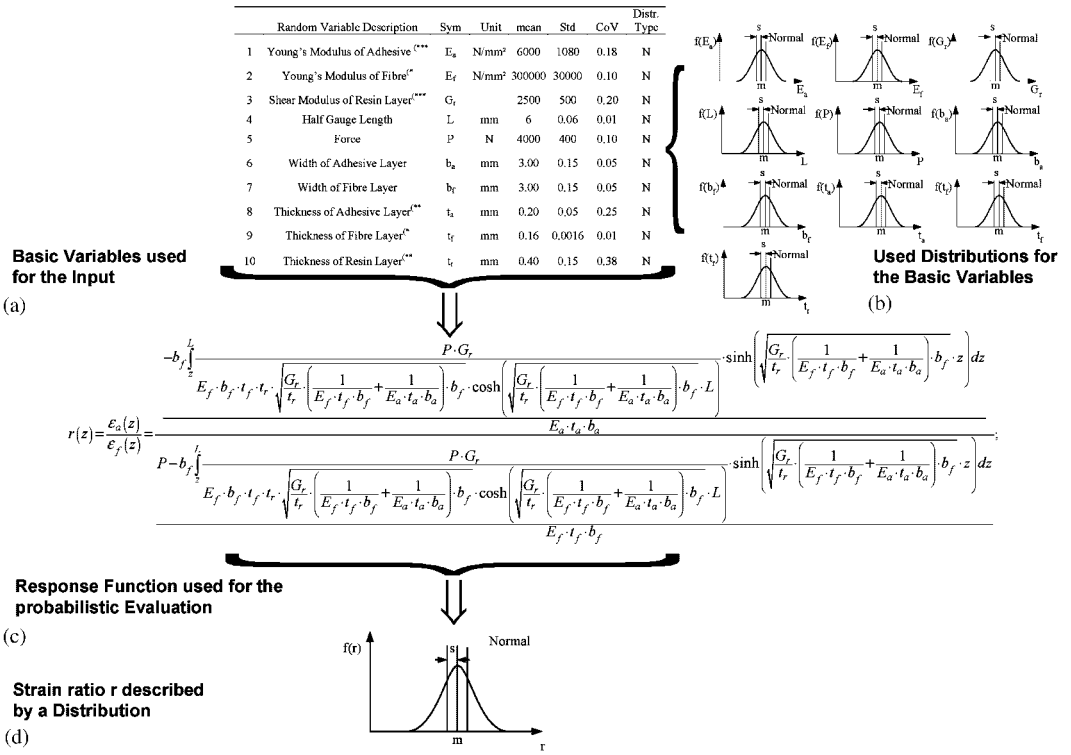

Figure 4. Concept of probabilistic modelling.

found, which participate authoritatively in the result, see Figure 5. For this problem there is a very suitable tool within probabilistic theory—sensitivity analysis. This delivers the participation of the random variables, in the form of weighting factors α_i in the result. These weighting factors are therefore deciding factors at the attempt to minimise the uncertainties. In the following paragraphs the statistical theory for the reliability analysis is repeated to show the development of the response function and the weighting factors α_i regarding our problem.

3.2. Theoretical model for the statistical sensitivity analysis

3.2.1. Formulation of the limit state function: sensitivity factors. Ernst Basler [9] developed the method of limit state formulation as described by Cornell [10]. The limit state function $G = R - S$ is the origin of this formulation. The variables R and S are random and are described by the mean value (μ_R, μ_S) and the standard deviation (σ_R, σ_S). In fact, G is the so-called safety margin $M = R - S$, see Figure 6.

The margin is created as the sum of two normal distributed variables R and S, therefore M is also distributed normally. The statistical values of M are obtained by simple algebra, see Figure 6. The safety index β is defined as μ_M/σ_M, it shows how often the standard deviation of M may be placed between zero and the mean value of M, see Figure 6. The probability of failure

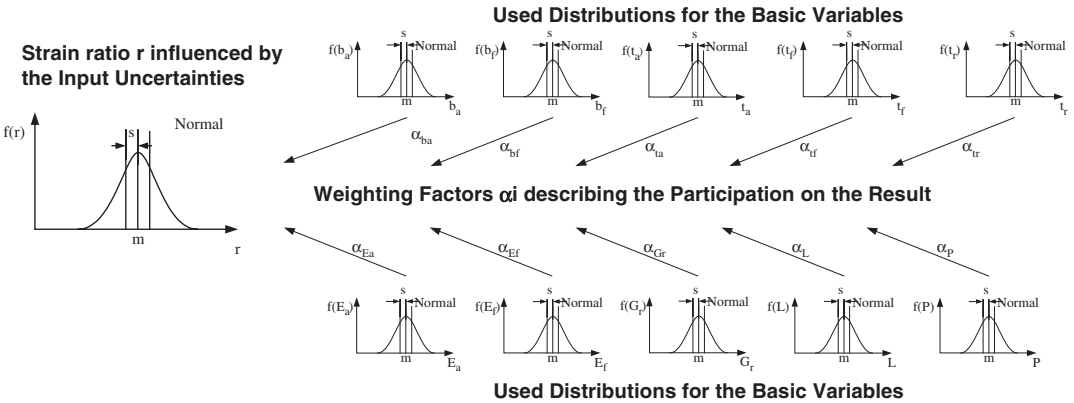

Figure 5. Participation of the random variables in the result.

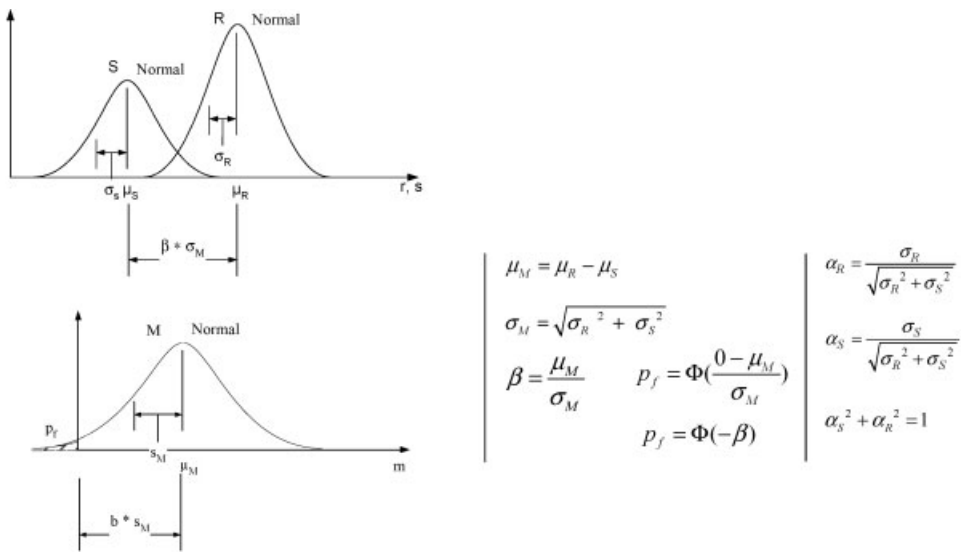

Figure 6. R, S, M and the safety index β.

$p_f = P(R - S < 0)$ is obviously the same as the probability that M is smaller than zero $p_f = P(M < 0)$. The probability of failure of the response function for this problem can be recognised as an index of the measuring inaccuracy.

The weighting factors α_i indicate the extent that the corresponding variable participates in the value of the probability of failure. In Figure 6 the derivation for two variables is shown. This kind of formulation of the safety problem allows one to create a simple design condition, $\mu_R - \beta_0 \alpha_R \sigma_R \geqslant \mu_S + \beta_0 \alpha_S \sigma_S$, where the participation of the uncertainties can also be considered.

For a limit state function containing more than two independent variables the formulation in Equation (13) is valid. It is a simple extension of the two-dimensional case. A transformation of the problem in normalised space provides a better algorithm from the computational point of view, see Equations (14)–(17). They show the definition of the statistical elements for a linear limit state function containing more than two independent variables. Examples for the determination of the linear combination coefficients b_i can be found elsewhere [11]. Of special interest for our problem is the definition of the weighting factors α_i in Equation (17). This equation shows the general concept for the calculation of the weighting factors α_i.

$$G = b_0 + \sum_{i=1}^{n} b_i X_i = 0 \tag{13}$$

$$\mu_G = b_0 + \sum_{i=1}^{n} b_i \mu_i \tag{14}$$

$$\sigma_G = \left[\sum_{i=1}^{n} (b_i \sigma_i)^2 \right]^{1/2} \tag{15}$$

$$\beta = \frac{\mu_G}{\sigma_G} \qquad \rightarrow p_f = \Phi(-\beta) \tag{16}$$

$$\alpha_i = \frac{\sigma_i}{\sigma_G} b_i \left(\sum_{i=1}^{n} \alpha_i^2 = 1 \right) \tag{17}$$

3.2.2. Our problem definition in the context of limit state functions. The limit state formulation $G = R - S$ contains the two variables R and S. In our case the equation has been reduced to one variable R. However this variable R, describing the strain ratio $\varepsilon_a(z)/\varepsilon_f(z)$, contains ten random variables as shown in Equation (12). This equation is not obviously a linear combination, therefore the formula apparatus for the linear state function, as described before, is not valid. One way to overcome this problem is the use of the first-order, second-moment (FOSM) method. The basic idea is the same as for the linear function, only the formulations are related to the nonlinear limit state function. For a more detailed description see Schneider [11]. For the problem in question, the VaP software [8] was used for the FOSM method.

3.2.3. VaP Software. The program VaP (Variables Processor) processes stochastically defined numerical quantities X_i, so-called variables, in given algebraically defined functions $G(X_i)$. It solves primarily computational problems arising in the reliability theory, but additionally it allows quite generally the investigation of the effects of variables and therefore is a useful tool in decision processes. VaP computes the expectation, the standard deviation and, if applicable, higher moments of G. It shows the shape of the probability density function of G, and calculates the probability that G is less than zero. In these investigations the response functions are formulated in VaP and the statistic moments are assigned to the defined basic variables (Table II). As an output the result of the response function is obtained in the form of statistical moments and the participation of the basic variables on the result are shown in the form of

Table II. Basic variables X_i of $r = (\varepsilon_a/\varepsilon_f)$.

Random variable		Symbol	Unit	Mean	Std	CoV	Type
1	Young's modulus of adhesive***	E_a	N/mm^2	6000	1080	0.18	Normal
2	Young's modulus of fibre*	E_f	N/mm^2	300 000	30 000	0.10	Normal
3	Shear modulus of resin layer***	G_r		2500	500	0.20	Normal
4	Half gauge length	L	mm	6	0.06	0.01	Normal
5	Force	P	N	4000	400	0.10	Normal
6	Width of adhesive layer	b_a	mm	3.00	0.15	0.05	Normal
7	Width of fibre layer	b_f	mm	3.00	0.15	0.05	Normal
8	Thickness of adhesive layer**	t_a	mm	0.20	0.05	0.25	Normal
9	Thickness of fibre layer*	t_f	mm	0.16	0.0016	0.01	Normal
10	Thickness of resin layer**	t_r	mm	0.40	0.15	0.38	Normal

*Literature. FOSM analysis VaP; $E_a = 6000\ N/mm^2$, $t_r = 0.40$ mm, $L = 6.00$ mm.
**Experimental data.
***Estimate.

weighting factors α_i. For more, an additional smart software in the probabilistic field is reported in Pukl *et al*. [14].

3.3. *Statistical parameters of the strain ratio as a function of distance of the symmetric axis*

In this section the behaviour of the electrical strain gauge, and in particular the variation of the ratio $r = \varepsilon_a/\varepsilon_f$ along the longitudinal axis is considered more specifically. The examination is performed on an example with a gauge length of $2L = 13$ mm, a resin thickness of $t_r = 0.4$ mm and a Young's modulus of the adhesive at $E_a = 6000\ N/mm^2$. The basic variables describing the example in a stochastical way are listed in Table II. It can be seen that all the basic variables are supposed to be normally distributed and independent. The normal distribution seems to be an accurate assumption for the first approximation, owing to the central limit theorem [12]. A further assumption is that the basic variables are independent. This assumption has to be made because of the information of the correlation between the variables is not completely available. From the experimental results of Ghini [7] the variation coefficient of the adhesive layer thickness is of about 38%. This value is taken into account, as can be seen from Table II, in the following considerations. In the following paragraphs the symbol m is used for mean, std is used for standard deviation, CoV is for coefficient of variation, skew for skewness and "kot" is used for kurtosis.

The basic variables are the input data for the software package VaP, [8]. They are taken into account with the statistical properties, mean value and standard deviation—Second moment—and the distribution type. The software allows the formation of the limit state function as described before. The limit state function, which is the kernel of a probabilistic formulation, includes all the basic variables of Table II and is derived from the mathematical model of Bonfiglioli *et al*. [3]. The inclusion of the variable z (distance from the axis of symmetry of the strain gauge) in the mathematical model is performed successfully by the software Mathematica. The judgement of the mechanical model with the FOSM method of VaP provides the mean value, standard deviation, skewness and kurtosis of the response. These evaluations are made at points of interest. The points with $z = 3.0, 4.5, 5.0, 5.6$ and 5.9 mm were selected as interesting points of the gauge with the length $2L = 6$ mm for detailed observation. At the point $z = 3.00$ mm an abnormality of the strain ratio r from 1 is at first

Table III. Distribution characteristics of $r = (\varepsilon_a/\varepsilon_f)$.

z (mm)	3.0	4.5	5.0	5.6	5.9
m	0.997 776	0.963 422	0.897 759	0.614 868	0.211 158
std	0.003 482	0.031 412	0.062 619	0.119 766	0.134 603
skew	−1.876 430	−1.237 660	−0.688 216	0.314 222	0.171 435
kot	5.038 250	3.440 360	2.906 650	3.039 470	3.046 600
CoV	0.003 490	0.032 604	0.069 750	0.194 783	0.637 452

$E_a = 6000\ \mathrm{N/mm^2}$, $t_r = 0.40$ mm, $L = 6.00$ mm.

clearly observable, see Table III. At the point $z = 5.6$ mm the abnormality of the strain ratio r is in an operable domain, the mean value coincides very well with the deterministic mathematical model and with the results of the FEM analysis ATENA. A comparison of the mean values of Table III with the values in Figures 7(a) and (b) shows the correctness of this statement, (for $n\Delta u = 5$–15). At the point $z = 5.9$ mm the mean value shows a dramatic reduction and the scattering attains a high value. It can be assumed that this point is not in an operable domain.

ATENA is a FEM software package for the calculation of nonlinear problems. This software permits the choice of highly developed material models for concrete and for other materials, and offers the possibility of individual customisation of the models. The software offers besides the material model, relatively elegant possibilities for the solution to bonding and debonding problems. These qualities were the prime reason for the choice of ATENA for the examination of the problem with different materials. Figure 7(c) shows one of the simulation results used for examination of agreement.

Yuan *et al.* [13] have already reported on the uniqueness at the end of the strain gauges. Their explanation concerning the effective length of strain gauges and consideration of electrical strain gauges with a polyamide foil which includes the electrical resistance (grid) leads to the treatment of the grid length as an effective length and the foil length as the total length, see Figure 8.

The sensitivity analysis, i.e. the designation of the weighting factors α_i of the basic variables, is also carried out with the software package VaP. It provides us with insight into the participation of a basic variable in the result. The results obtained are shown in Table IV. We can see that the length of the gauge is the authoritative factor followed by the resin thickness, adhesive thickness, modulus of elasticity of adhesive and the shear modulus of resin.

In addition more detailed analyses are executed to find out the behaviour of the statistical parameters as a function of the resin thickness. The parameters of the model are kept constant, except for the mean value of the resin thickness. Figure 9 shows the mean values of the strain ratio r as a function of resin thickness t_r and the distance z from the centre of the electrical strain gauge. It has been mentioned that the mean values decrease with increasing z. The decrease is moderate until $z = 5.6$ mm and then exceeds this value progressively. This behaviour of the mean values is highlighted with increasing thickness of resin, see Figure 9. The mean value of the strain ratio for the resin thickness $t_r = 0.1$ mm at $z = 3$ mm is 0.999 and for resin thickness 1.0 mm it is 0.980. The corresponding values at $z = 4.5$ mm (effective length) are 0.997 and 0.887. This obvious effect points out the significance of the resin thickness beyond the gauge length. In Section 3.4 the analysis of the weighting factors α_i in the context of the resin thickness and Young's modulus of adhesive will be discussed in more detail.

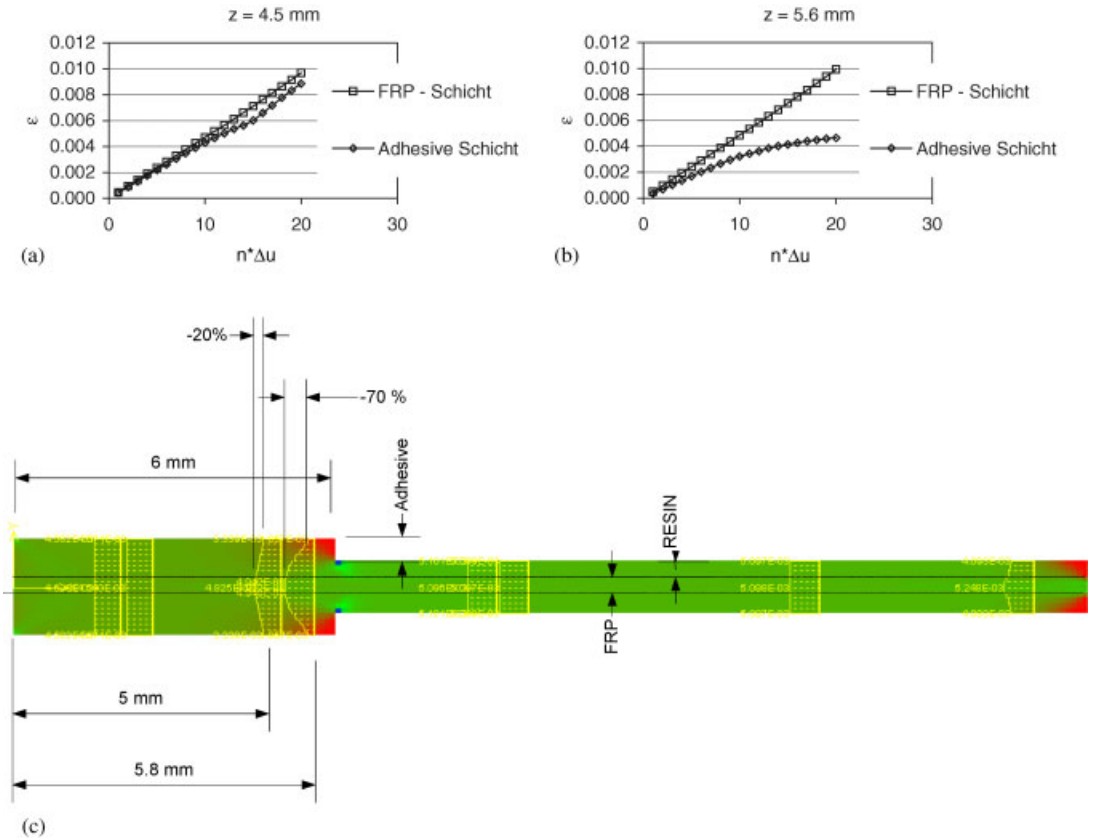

Figure 7. (a, b) Strain curves as a function of the deformations obtained from the FEM analysis: n = number of loadsteps, Δu = displacement per loadstep (c) results from FEM for $E_a = 6000\ \mathrm{N/mm^2}$, $t_r = 0.40$ mm, $L = 6.00$ mm, $n\Delta u = 10$.

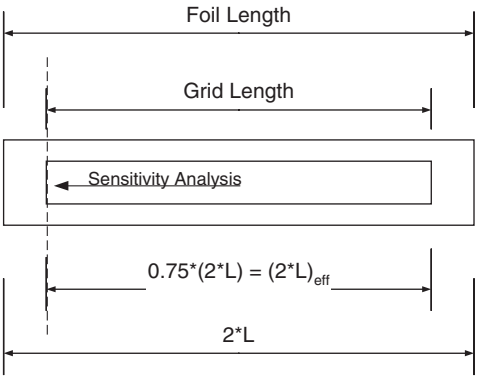

Figure 8. Electrical strain gauge; definition of the effective length.

Table IV. Weighting factors α_i of $r = (\varepsilon_a/\varepsilon_f)$.

E_a	E_f	G_r	L	P	b_a	b_f	t_a	t_f	t_r
0.0020	0.0000	0.0020	1.0000	0.0000	0.0006	0.0006	0.0030	0.0000	0.0040

$E_a = 6000\ \mathrm{N/mm^2}$, $t_r = 0.40$ mm, $L = 6.00$ mm.

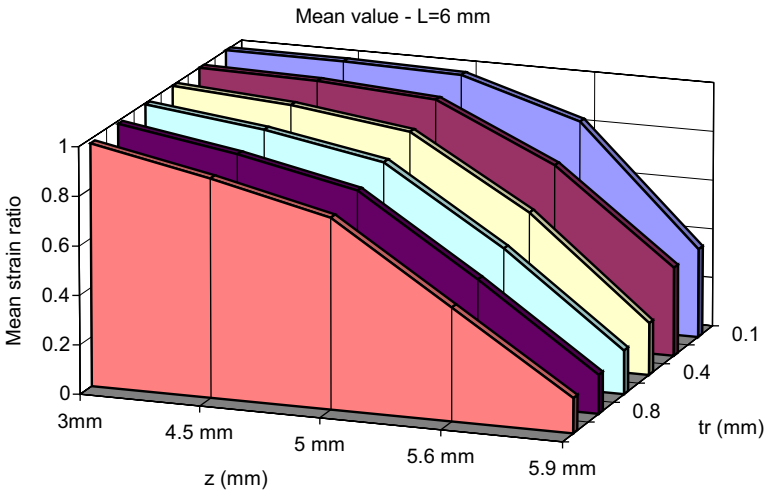

Figure 9. Mean values of ESG with a different thickness t_r of resin; gauge length $L = 6.00$ mm.

From Figure 10 the behaviour of the standard deviation of the strain ratio r can be deduced. The standard deviation increases with increasing distance z and with increasing resin thickness t_r. Furthermore it can be seen that the standard deviations increases tremendously at the end of the strain gauge. This effect can even be observed for a resin thickness of 0.1 mm, and is more pronounced as z and t_r increase.

3.4. Statistical parameters the strain ratio as a function of the resin thickness

The objective of this section is to illustrate the sensitivity of the basic variables, chosen for the above mentioned probabilistic model. The sensitivity is described by the weighting factors α_i. This investigation sets out to extend the study carried out in Bonfiglioli *et al.* [3]. The examination is based on Table II. At the first step values 0.4, 0.6 and 0.8 mm are assumed for the resin thickness, and the values 3000, 6000, 9000, and 12000 $\mathrm{N/mm^2}$ for Young's modulus of the adhesive.

In Figure 11 both mean values and the standard deviations of the strain ratio resulting from the different values of the resin thickness are plotted against the Young's modulus of the adhesive. It is evident from Figure 11 and Table V that the mean values of the strain ratio decrease with increasing thickness of resin and increasing Young's modulus of an adhesive. The mean values for the investigated domain of the resin thickness and the domain of Young's modulus of adhesive range between 0.826 and 0.989 (16.5%). From Figure 11 and Table V it is also seen that the standard deviation increases with the increase of the resin thickness, as

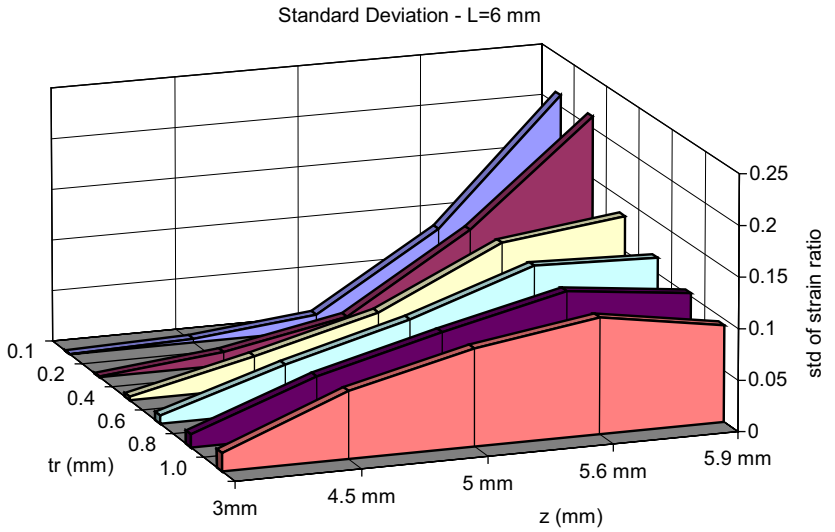

Figure 10. Standard deviation values of ESG with a different thickness t_r of resin; gauge length $L = 6.00$ mm.

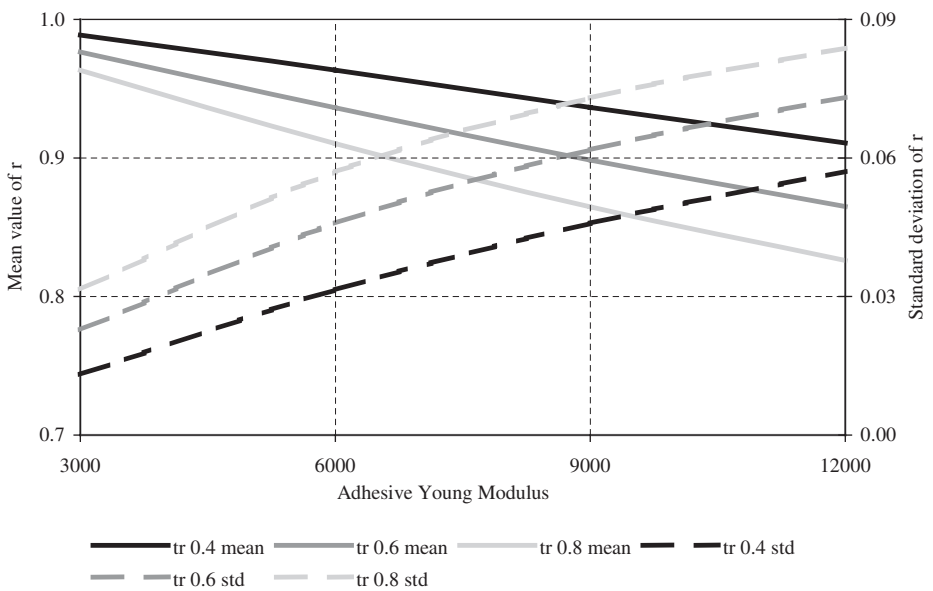

Figure 11. Strain ratio as a function of Young's modulus of the adhesive for different values of the resin thickness; gauge length $L = 6.00$ mm.

mentioned in Section 3.3, and the increase of Young's modulus of the adhesive. The coefficient of variation ranges between 0.013 and 0.101 (87%) for the considered resin thicknesses and Young's modulus of the adhesive (or $\sim$ 30% for a fixed Young's modulus of the adhesive).

Table V. Distribution characteristics of $r = (\varepsilon_a/\varepsilon_f)$.

E_a	x	Mean	skew	kot	CoV
$t_r = 0.40$ mm					
3000	4.5	0.989	−1.581	3.965	0.013
6000	4.5	0.963	−1.238	3.440	0.033
9000	4.5	0.937	−0.966	3.156	0.049
12000	4.5	0.911	−0.758	2.987	0.063
$t_r = 0.60$ mm					
3000	4.5	0.977	−1.398	3.648	0.023
6000	4.5	0.936	−0.960	3.148	0.049
9000	4.5	0.898	−0.663	2.924	0.069
12000	4.5	0.865	−0.454	2.817	0.085
$t_r = 0.8$ mm					
3000	4.5	0.963	−1.231	3.428	0.033
6000	4.5	0.910	−0.746	2.978	0.063
9000	4.5	0.865	−0.448	2.816	0.084
12000	4.5	0.826	−0.249	2.759	0.101

FOSM analysis VaP; gauge $L = 6.00$ mm.

For example, if we use an adhesive with Young's modulus of 6000 MPa and the thickness of the resin layer is 0.6 mm, assuming an actual strain of the composite of 1000 micro-strain, we can expect a measured value of the strain between 885 and 1040 micro-strain, with a probability of 90%.

In a further step, the participation of the basic variables in the results are of interest. With the use of the response function (Equation 12), and FOSM theory, performed with the software VaP, the following distribution of the weighting factors α_i is obtained. The length of the gauge is the most important influencing factor, followed by the resin thickness t_r, the adhesive thickness t_a, the shear modulus of resin layer G_r and Young's modulus of adhesive E_a. As a result of the dominant character of the gauge length in this observation—the weighting factor is several times greater than the others—in the percentage comparison of the weighting factors the gauge length is excluded. Figure 12 shows that the resin thickness t_r participates to $\sim$ 30%, the adhesive thickness t_a $\sim$ 25% followed by the shear modulus of resin G_r $\sim$ 20% and Young's modulus of adhesive E_a $\sim$ 17%.

Further investigations of the weighting factors α_i showed that there is no significant influence of the thickness of resin and Young's modulus of the adhesive on the percentage ranking. This constant behaviour of the α_i can be justified by the dominant character of the gauge length.

3.5. Statistical parameters of the strain ratio as a function of the gauge length

In this section, the effect of the gauge length on the statistical parameters and on the weighting factors α_i is discussed in detail. The basis of the investigation is the probabilistic model and the basic variables of Table II. First, the mean values of the gauge length (3, 6 and 10 mm), and the mean values of Young's modulus of the adhesive (3000, 6000, 9000 and 12,000 N/mm^2) are varied.

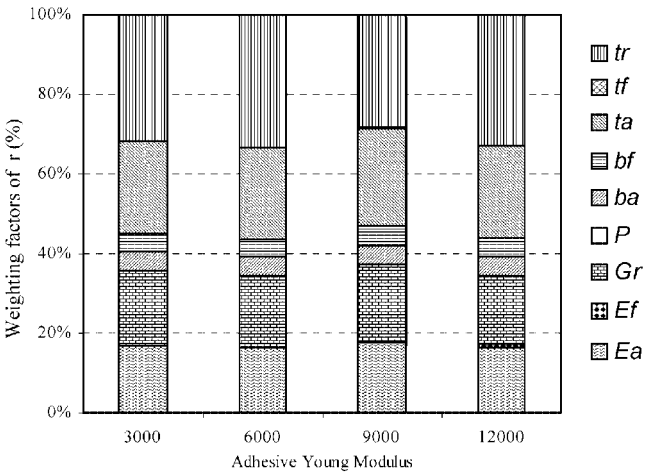

Figure 12. Distribution of the weighting factors α_i for different Young's modulus of the adhesive and values of the resin thickness.

In Figure 13 the strain ratio resulting from the different gauge lengths are plotted against Young's modulus of the adhesive. Figure 13 and Table VI show that the mean values of the strain ratio decreased with decreasing gauge length and increasing Young's modulus of the adhesive. The mean values for the investigated domain of the gauge length and the domain of the Young's modulus of adhesive range between 0.814 and 0.997 (18%), see Table V. Figure 13 shows that the standard deviation increases with the decrease of the gauge length and the increase of Young's modulus of the adhesive. The coefficient of variation ranges between 0.005 and 0.229 (98%) for the considered gauge length and Young's modulus of adhesive (or $\sim$ 16% for a fixed Young's modulus of adhesive). 'It can be clearly seen that short gauges are to be avoided for application on resin coating' [3]. This statement must be emphasised. In the same way as in Section 3.4 the distribution of the weighting factors α_i is determined. The length of the gauge is still the most important influencing factor followed by the resin thickness t_r, adhesive thickness t_a, shear modulus of resin layer G_r and Young's modulus of the adhesive E_a. For the same reason as stated previously, the percentage comparison of the weighting factors was made without the gauge length. The resin thickness t_r participates to $\sim$ 34%, the adhesive thickness t_a to $\sim$ 23% followed by the shear modulus of resin G_r $\sim$ 18% and Young's modulus of adhesive E_a $\sim$ 17%. With reference to Section 3.4 it can be seen that the percentage distribution and the ranking of the weighting factors α_i do not differ greatly. The ranking is similar to that in Figure 12. As mentioned above, the dominant character of the gauge length is still apparent.

4. DEVIATION OF THE GAUGE FROM THE LONGITUDINAL AXIS

Until now, the investigations conducted on the probabilistic model are based on the assumption that the electrical strain gauges are bonded exactly in the longitudinal direction on the FRP. Experience demonstrates that this is not usually the case, because handling these small elements is sometimes difficult, particularly if the application has to be performed in an existing

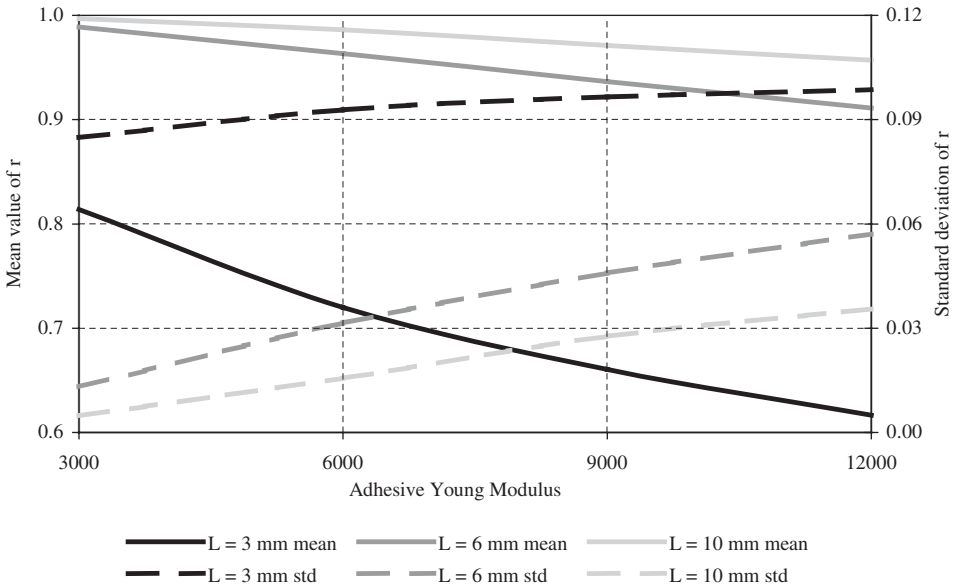

Figure 13. Strain ratio as a function of Young's modulus of the adhesive for different values of the gauge length resin thickness $t_r = 0.4$ mm.

Table VI. Distribution characteristics of $r = (\varepsilon_a/\varepsilon_f)$.

E_a	x	Mean	skew	kot	CoV
$L = 3$ mm					
3000	2.3	0.814	−0.305	3.698	0.152
6000	2.3	0.720	0.089	3.552	0.189
9000	2.3	0.660	0.297	3.532	0.212
12000	2.3	0.617	0.427	3.547	0.229
$L = 6$ mm					
3000	4.5	0.989	−1.581	3.965	0.013
6000	4.5	0.963	−1.238	3.440	0.033
9000	4.5	0.937	−0.966	3.156	0.049
12000	4.5	0.911	−0.758	2.987	0.063
$L = 10$ mm					
3000	8.0	0.997	−1.703	4.233	0.005
6000	8.0	0.986	−1.523	3.759	0.016
9000	8.0	0.971	−1.343	3.502	0.028
12000	8.0	0.957	−1.179	3.318	0.037

FOSM analysis VaP; resin $t_r = 0.40$ mm.

strengthened structure. Therefore uncertainties in positioning the electrical strain gauges cannot be prevented. It is therefore very important to know how much the deviation of the direction of the electrical strain gauges from the longitudinal axis of the FRP affects the strain measurement.

Thus, the model used to evaluate the strain ratio, Equation (18), has to be extended to include the uncertainties in the deviation.

$$r = \frac{\varepsilon_a}{\varepsilon_f} \tag{18}$$

For the plane strain situation (Figure 14) the following equation can be derived, with the following symbols: ε_L = strain in longitudinal direction of the gauge, ε_T = strain in perpendicular direction; $\gamma_{LT} = 2 \times$ shear − strain of the gauge; ε_x = strain in longitudinal direction of laminate; ε_y = strain in perpendicular direction; $\gamma_{xy} = 2 \times$ shear − strain of the laminate; Θ = angle of gauge deviation.

$$\begin{Bmatrix} \varepsilon_L \\ \varepsilon_T \\ \frac{1}{2}\gamma_{LT} \end{Bmatrix} = \begin{bmatrix} \cos^2\Theta & \sin^2\Theta & 2\sin\Theta\cos\Theta \\ \sin^2\Theta & \cos^2\Theta & -2\sin\Theta\cos\Theta \\ -\sin\Theta\cos\Theta & \sin\Theta\cos\Theta & \cos^2\Theta - \sin^2\Theta \end{bmatrix} \begin{Bmatrix} \varepsilon_x \\ \varepsilon_y \\ \frac{1}{2}\gamma_{xy} \end{Bmatrix} \tag{19}$$

or in general terms

$$\varepsilon' = T\varepsilon \tag{20}$$

Under the assumption of a homogeneous strain field, when the laminate is subject to a uniaxial longitudinal stress state, we obtain the strain in the direction of the gauge

$$\varepsilon_L = \varepsilon_x \cos^2\Theta + \varepsilon_y \sin^2\Theta = \varepsilon_x(\cos^2\Theta + v\sin^2\Theta) \tag{21}$$

In Equation (21), the term in $\sin^2\Theta$ commas is much smaller than the previous term, so we can write

$$\varepsilon_L = \varepsilon_x \cos^2\Theta \tag{22}$$

The modified form for the strain ratio is finally obtained

$$r = \frac{\varepsilon_a \cos^2\Theta}{\varepsilon_f} \tag{23}$$

4.1. Statistical parameters of the strain ratio as a function of the gauge deviation

The contents of this section examine the influence of the strain error due to the deviation of the gauge from the longitudinal direction of the laminate. The values of Table II are the basis for this discussion. Regarding Equation (23) in a probabilistic manner, numerous angles of

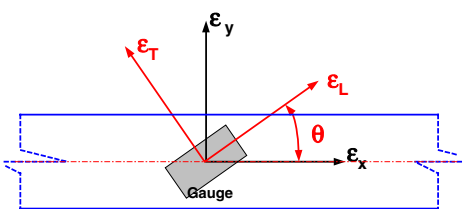

Figure 14. Strain transformation.

deviation described by two statistical parameters, mean value and standard deviation, are evaluated. Figure 15 and Table VII show three of these results. As expected the decrease of the mean values is linked with the increase of the angle values and the increase of Young's modulus of the adhesive.

The results of the angle with a mean value of 9° and a standard deviation of 7° (Figure 15 and Table VII) have a particular meaning. Until this value of the angle is reached, the sensitivity analysis, i.e. the ranking of the weighting factors α_i, shows a similar behavior as in Sections 3.4 and 3.5, see Figure 12, where the participation of the angle on the result increases gradually, in the region of 9° a progressive increase of the weighting factor of the angle is observed, see Figure 16. In these illustrations, at the value $E_a = 3000$ MPa of Young's modulus of the adhesive the weighting factor has already assumed a large value. The weighting factor α_i for the other values of E_a is still in the range of the α_i of t_r, t_a, G_r and E_a. However, a small increase of the mean value or the standard deviation of the angle leads to the same behavior of the α_i for the other E_a. This allows the conclusion that the angle with a mean value of 9° and a standard deviation of 7° is in a critical range where the angle assumes the same authoritative character as the gauge length.

5. CONCLUSIONS

The effective length is most important for the variation of the strain ratio r and it can be defined at 0.75 of the gauge length $2L$. The sensitivity analysis shows that the length of the gauge is the

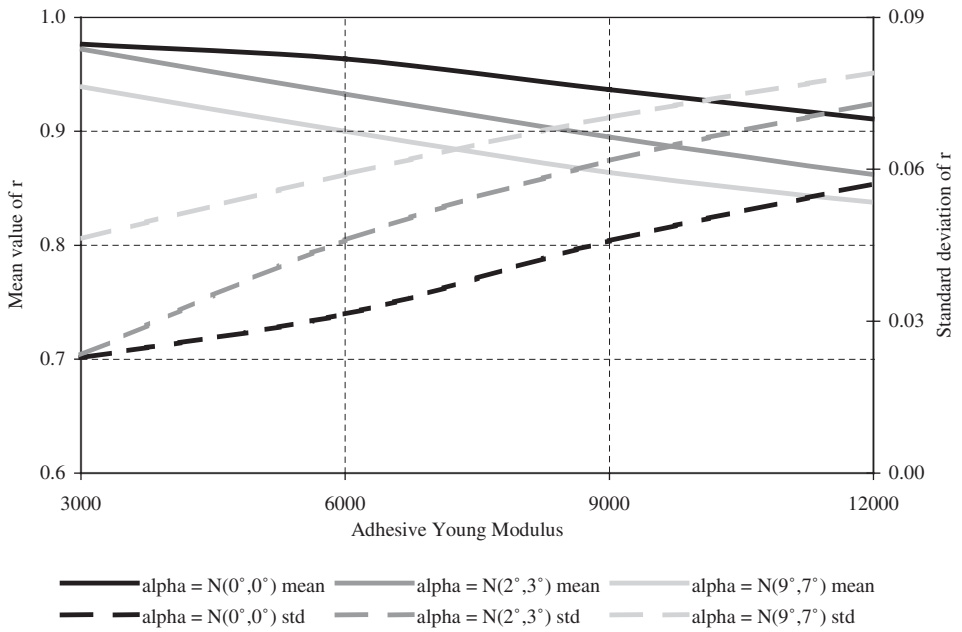

Figure 15. Strain ratio as a function of Young's modulus of the adhesive for different values of the gauge deviation; resin thickness $t_r = 0.4$ mm; gauge $L = 6.00$ mm.

Table VII. Distribution characteristics of $r = (\varepsilon_a/\varepsilon_t)$.

E_a	x	Mean	skew	kot	CoV
$\alpha = N(0;0)$					
3000	4.5	0.977	−1.398	3.674	0.013
6000	4.5	0.963	−1.238	3.440	0.033
9000	4.5	0.937	−0.966	3.156	0.049
12000	4.5	0.911	−0.758	2.987	0.063
$\alpha = N(2;3)$					
3000	4.5	0.972	−1.226	2.903	0.024
6000	4.5	0.933	−0.942	2.927	0.049
9000	4.5	0.895	−0.667	2.821	0.069
12000	4.5	0.862	−0.462	2.762	0.085
$\alpha = N(9;7)$					
3000	4.5	0.939	−1.188	3.085	0.049
6000	4.5	0.900	−0.799	2.631	0.066
9000	4.5	0.864	−0.589	2.636	0.081
12000	4.5	0.837	−0.425	2.673	0.094

FOSM analysis VaP; $t_r = 0.40$ mm, $L = 6.00$ mm.

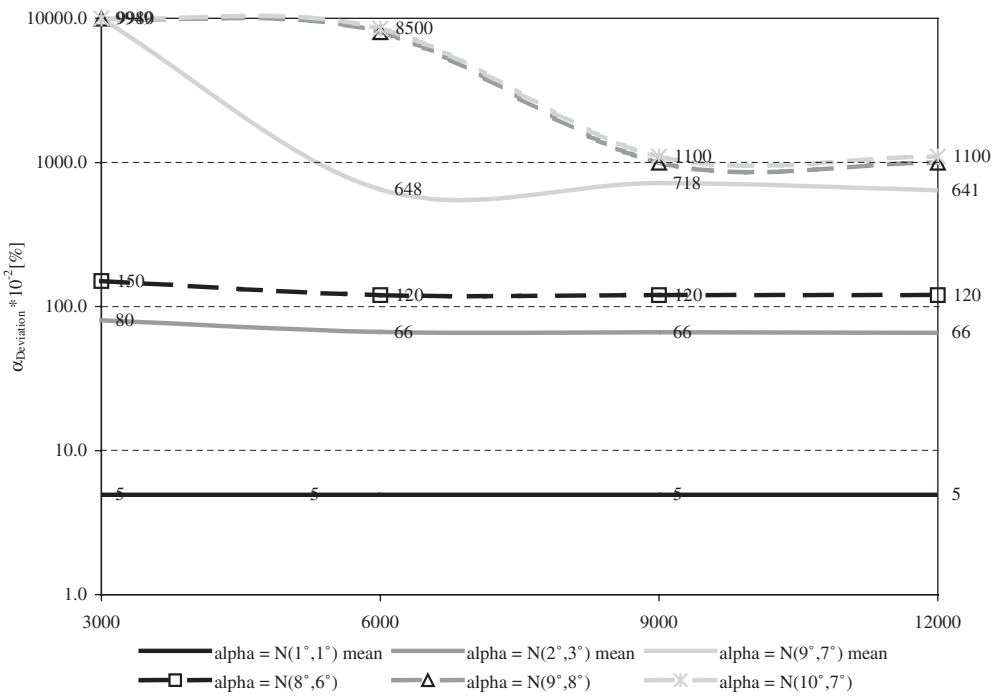

Figure 16. Weighting factor α_i of the deviation as a function of Young's modulus of the adhesive, resin thickness $t_r = 0.4$ mm; gauge $L = 6.00$ mm.

most important influencing factor followed by the resin thickness t_r, adhesive thickness t_a, shear modulus of resin layer G_r and Young's modulus of the adhesive E_a. As a result of the dominant character of the gauge length (the weighting factor is a several times greater than the others) in the percentage comparison of the weighting factors the gauge length is excluded. The investigations show that the resin thickness t_r participates to $\sim$ 30%, the adhesive thickness t_a to $\sim$ 25% followed by the shear modulus of resin $G_r \sim 20\%$ and Young's modulus of the adhesive $E_a \sim 17\%$. The percentage distribution of the weighting factors α_i seems not to be influenced by the thickness of resin; it also seems not to be influenced by the different values of Young's modulus of the adhesive. This constant behaviour of α_i can be justified by the dominant character of the gauge length.

- The observation of the statistical parameters (mean, CoV) of the strain ratio as a function of the gauge length and of Young's modulus of the adhesive allows the following statement to be made—the mean values of the strain ratio reduce and the standard deviation increases with decreasing gauge length and increasing Young's modulus of the adhesive. So it is important to use gauges with an adequate length for application on resin coating.
- The observation of the statistical parameters (mean, CoV) of the strain ratio as a function of the gauge deviation and of Young's modulus of adhesive indicates that the mean values of the strain ratio decrease and the standard deviation increases with increasing gauge angle and increasing Young's modulus of the adhesive. The detailed observation of the weighting factors α_i shows that the angle with a mean value of 9° and a standard deviation of 7° is a critical range where the angle becomes the same authoritative character as the gauge length. This statement is valid regarding the basic variables of Table II.

REFERENCES

1. Bastianini F, Di Tommaso A, Pascale G. Ultrasonic non destructive assessment of bonding defects in composite structural strengthenings. *Composite Structures* 2001; **53**:463–467.
2. Bonfiglioli B, Pascale G, Martinez de Mingo S. Dynamic testing of reinforced concrete beams damaged and repaired with CFRP sheet. *Journal of Materials in Civil Engineering* (ASCE), in press.
3. Bonfiglioli B, Di Muro P, Pascale G. Reliability of strain measurements in FRP. *Proceedings of the Structural Health Monitoring*, *SHM-ISIS2002 Workshop*, 19–20 September 2002; 275–83.
4. Arduini M, Bonfiglioli B, Manfroni O, Pascale G. New applications of fiber optic sensors for structural monitoring. *Proceedings of the IABSE Symposium on 'Structures for the Future—The Search for Quality'*, Rio de Janeiro, 25–27 August 1999; pp 491–498.
5. Pascale G, Carli R, Bonfiglioli B, Arduini M. Bridge r.c. beams: repair and monitoring. *International Conference on Structural Faults and Repair* London, 13–15 July 1999.
6. Bonfiglioli B, Manfroni O, Pascale G. Fibre optic sensors: improvement of the application in FRP monitoring. *Proceedings of the 3rd International Conference on Advanced Composite Materials in Bridges and Structures*, Ottawa, 15–18 August 2000; pp 127–134.
7. Ghini R. *Bond Problems of Strain Sensors on FRP. Graduation Thesis*. University of Bologna. 2002 (in Italian).
8. Petschacher M. VaP 1.5. Institute of Structural Engineering IBK, ETH Zürich, Switzerland.
9. Basler E. Untersuchungen über den Sicherheitsbegriff von Bauwerken. *Schweizer Archiv für angewandte Wissenschaft und Technik* 1961; **4**.
10. Cornell AC. A probability based structural code 1969; *ACI Journal Proceedings* Vol. 66, 1969.
11. Schneider J. "*Sicherheit und Zuverlässigkeit im Bauwesen*". vdf Hochschulverlag AG, 1994, pp 71–96.
12. Papula L. "*Mathematik für Ingenieure und Naturwissenschaftler* Band 3, Vieweg: 2001, pp 430–432.
13. Yuan L, Zhou L, Wu J. Investigation of coated optical fiber strain sensor embedded in a linear strain matrix material. *Optics and Lasers in Engineering* 2001; **35**:251–260.
14. Pukl R, Strauss A. Probabilistic-based assessment of Concrete Structures Using Nonlinear Fracture Mechanics"; *ICASP9* 6–9 July: 2003.

